Supplementary Information (SI) for Energy Advances.
This journal is © The Royal Society of Chemistry 2024

Synthesis of N-Doped Zeolite-Templated Carbons via Depolymerized Oligomer Filling: Applications in EDLC Electrodes

Hiroyuki Itoi,[a] *Chika Matsuoka,*[a] *Ginga Saeki,*[a] *Hiroyuki Iwata,*[b] *Shinichiroh Iwamura,*[c,d] *Keigo Wakabayashi,*[e] *Takeharu Yoshii,*[e] *Hirotomo Nishihara,*[c,e] *and Yoshimi Ohzawa*[a]

[a] Department of Applied Chemistry, Faculty of Engineering, Aichi Institute of Technology, 1247 Yachigusa, Yakusa, Toyota, 470−0392, Japan

[b] Department of Electrical and Electronics Engineering, Aichi Institute of Technology, Yachigusa 1247, Yakusa-cho, Toyota 470-0392, Japan

[c] Advanced Institute for Materials Research (WPI-AIMR), Tohoku University, 2-1-1 Katahira, Aoba-ku, Sendai 980-8577, Japan

[d] 3DC Inc., 2-1-1 Katahira, Aoba-ku, Sendai 980-8577, Japan

[e] Institute of Multidisciplinary Research for Advanced Materials, Tohoku University, 2-1-1 Katahira, Aoba-ku, Sendai 980-8577, Japan

S1. Result of differential scanning calorimetry analysis for GlcNAc

Fig. S1 presents the differential scanning calorimetry (DSC) spectrum of GlcNAc, collected using a differential scanning calorimeter (DSC-60, Shimadzu). Because the DSC measurement is conducted in a closed system, the sample mass remains constant. Therefore, unlike the DTA spectrum of GlcNAc (Fig. 1d), the fusion and decomposition were observed as endothermic and exothermic peaks, respectively.

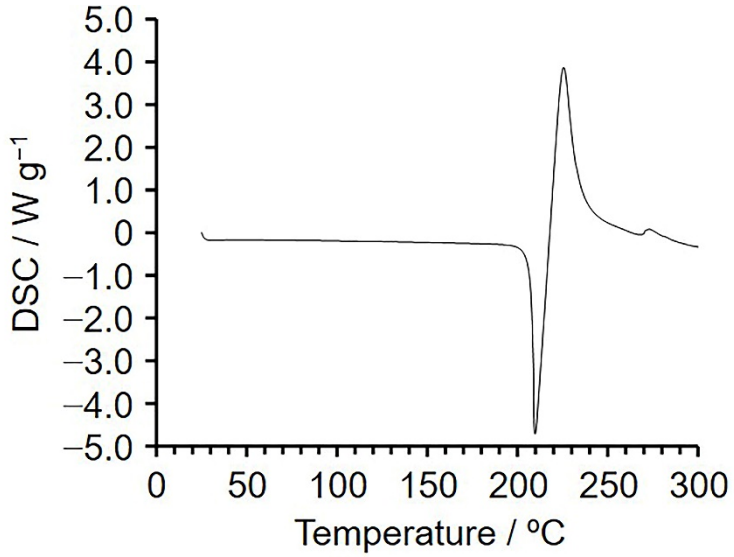

Fig. S1 DSC spectrum of GlcNAc (heating rate: 10 °C min^{-1}).

S2. Fitting results of DTA spectra without a Gaussian function

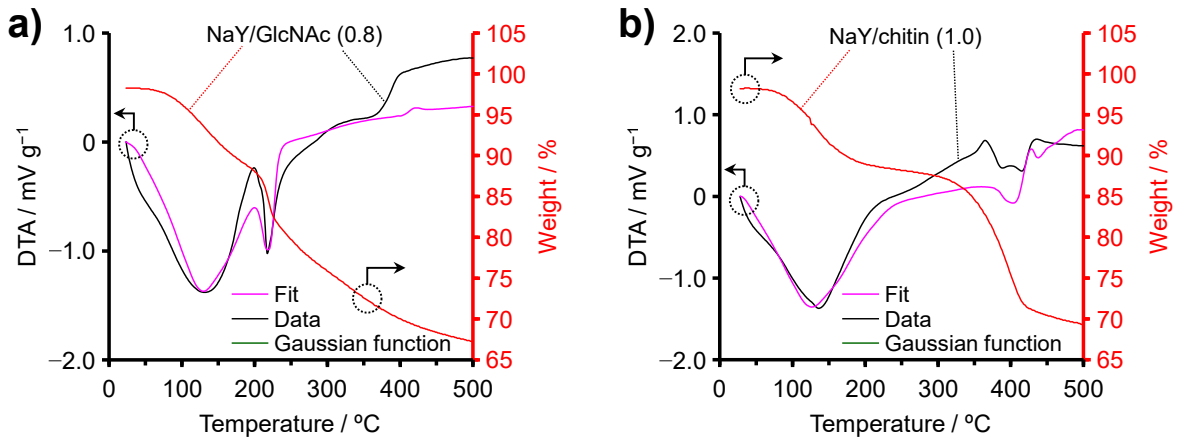

Fig. S2 Fitting results performed without a Gaussian function for the mixtures of (a) the zeolite and GlcNAc, and (b) the zeolite and chitin.

S3. Structural characterizations of G (2.0)-P, G (3.0)-P, and G (4.0)-P

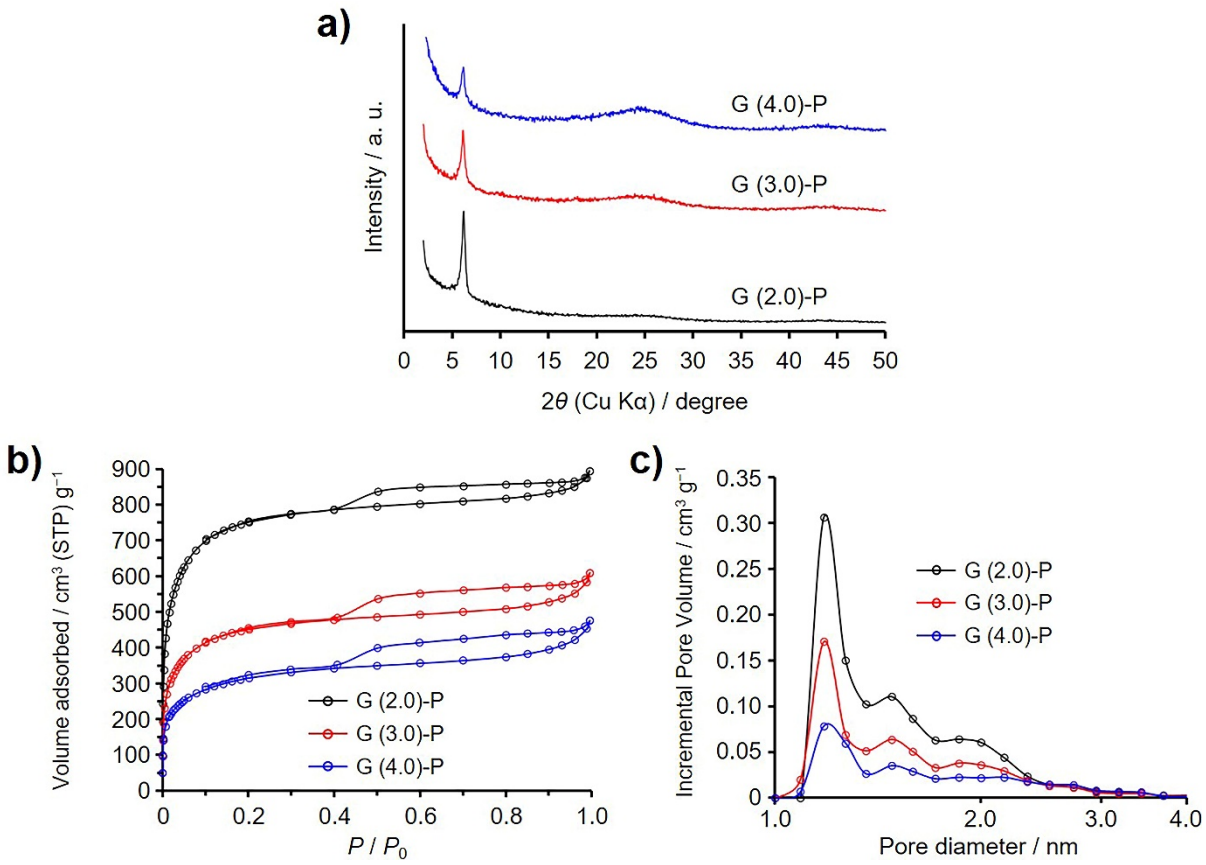

Fig. S3 Results of structural analyses on G (2.0)-P, G (3.0)-P, and G (4.0)-P. (a) XRD patterns. (b) N_2 adsorption/desorption isotherms. (c) Pore size distributions calculated by the DFT method (N_2, −196 °C, carbon slit pore model).

Table S1 BET Specific Surface Areas, Pore Volumes, and Carbon Fractions of ZTCs Prepared Using Propylene and Excess GlcNAc

Samples	S_{BET} ($m^2\ g^{-1}$)	V_{total} ($cm^3\ g^{-1}$)	V_{micro} ($cm^3\ g^{-1}$)	V_{meso} ($cm^3\ g^{-1}$)	Carbon fraction ($g\ g_{NaY}^{-1}$)
G (2.0)-P	2820	1.32	1.20	0.11	0.398
G (3.0)-P	1650	0.85	0.71	0.15	0.558
G (4.0)-P	1130	0.65	0.46	0.20	0.721

S4. SEM images of GlcNAc and the heated GlcNAc with propylene CVD and TEM images of G (4.0)-P

Fig. S4a displays the SEM image of GlcNAc, with particle sizes below 200 μm. Meanwhile, Fig. S4b presents the SEM image of GlcNAc treated under the same conditions as those used for the ZTC synthesis, but without NaY zeolite. The particle sizes in Fig. S4b are significantly larger than those in Fig. S4a, indicating that the GlcNAc particles melted and coalesced into larger particles during heating. Fig. S4c presents the TEM images of G (4.0)-P. Unlike the TEM images in Fig. 4b and 4d, thick carbon shells were observed on the outer surface of the ZTC particles.

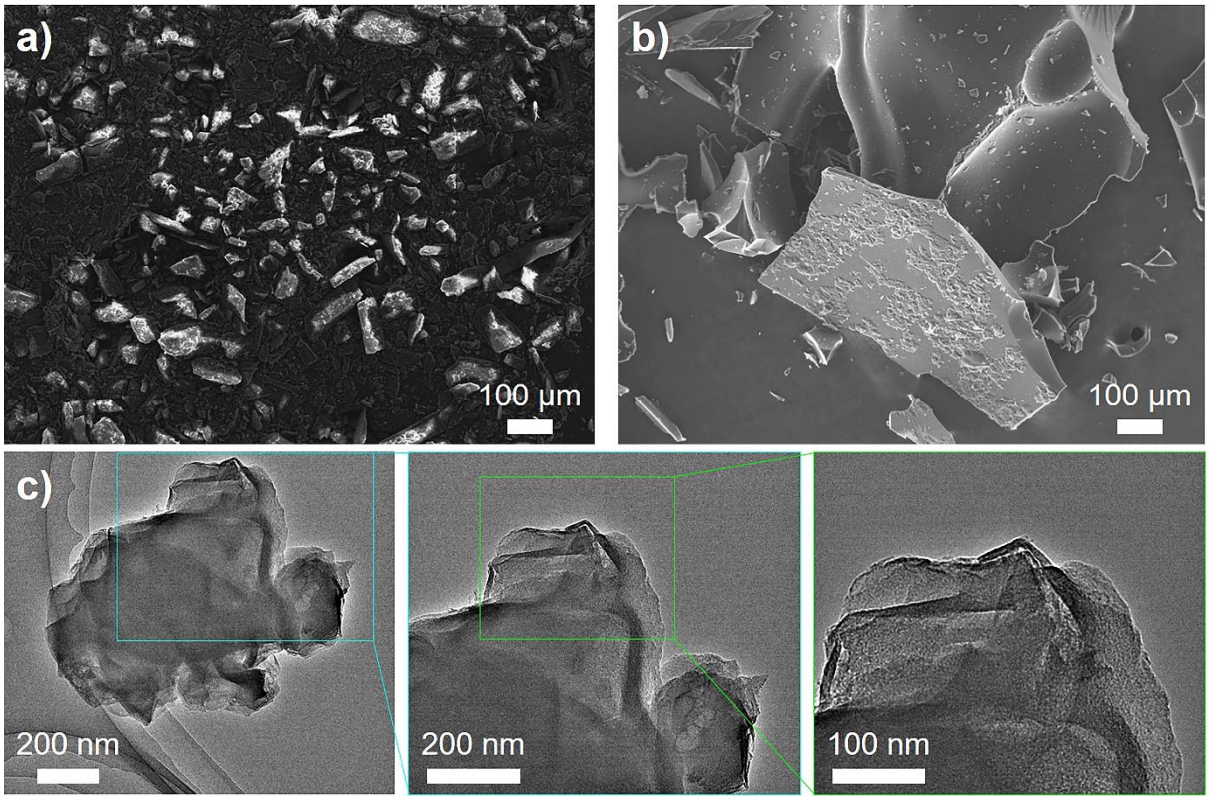

Fig. S4 SEM images of (a) GlcNAc and (b) the heated GlcNAc with propylene CVD. (c) TEM images of G (4.0)-P.

S5. Structural characterizations of heated GlcNAc and chitin without NaY zeolite

GlcNAc and chitin were treated under the same conditions as those used for ZTC synthesis, excluding the use of NaY zeolite. To investigate the effect of propylene CVD, treatments were performed both with and without propylene CVD, while maintaining the same temperature program for all samples. As shown in Fig. 5a, the chitin heated without propylene CVD exhibits both hysteresis and micropore filling, indicating the presence of both micropores and mesopores. Conversely, the chitin heated with propylene CVD showed almost no hysteresis or micropore filling, suggesting that the micropores and mesopores were filled with carbon during the CVD process. Regardless of whether propylene CVD was employed, the heated GlcNAc showed no porosity. Their XRD patterns, typical of amorphous carbons, are presented in Fig. S5b.

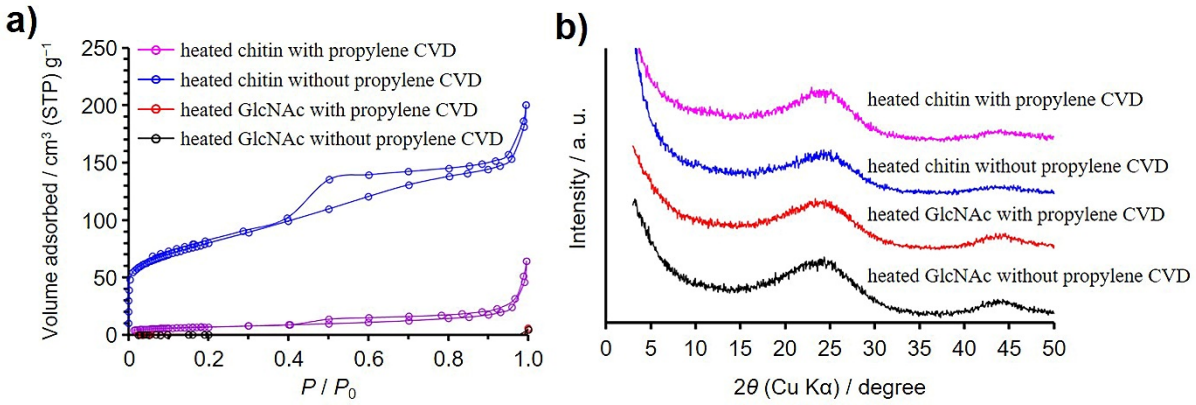

Fig. S5 (a) N_2 adsorption/desorption isotherms and (b) XRD patterns.

Table S2 BET Specific Surface Areas and Pore Volumes of Heated Chitins with and without Propylene CVD

Samples	S_{BET} ($m^2\ g^{-1}$)	V_{total} ($cm^3\ g^{-1}$)	V_{micro} ($cm^3\ g^{-1}$)	V_{meso} ($cm^3\ g^{-1}$)
heated chitin without propylene CVD	283	0.24	0.11	0.13
heated chitin with propylene CVD	25	0.04	0.01	0.03

S6. Structural characterizations of C (2.0)-P, C (3.0)-P, and C (4.0)-P

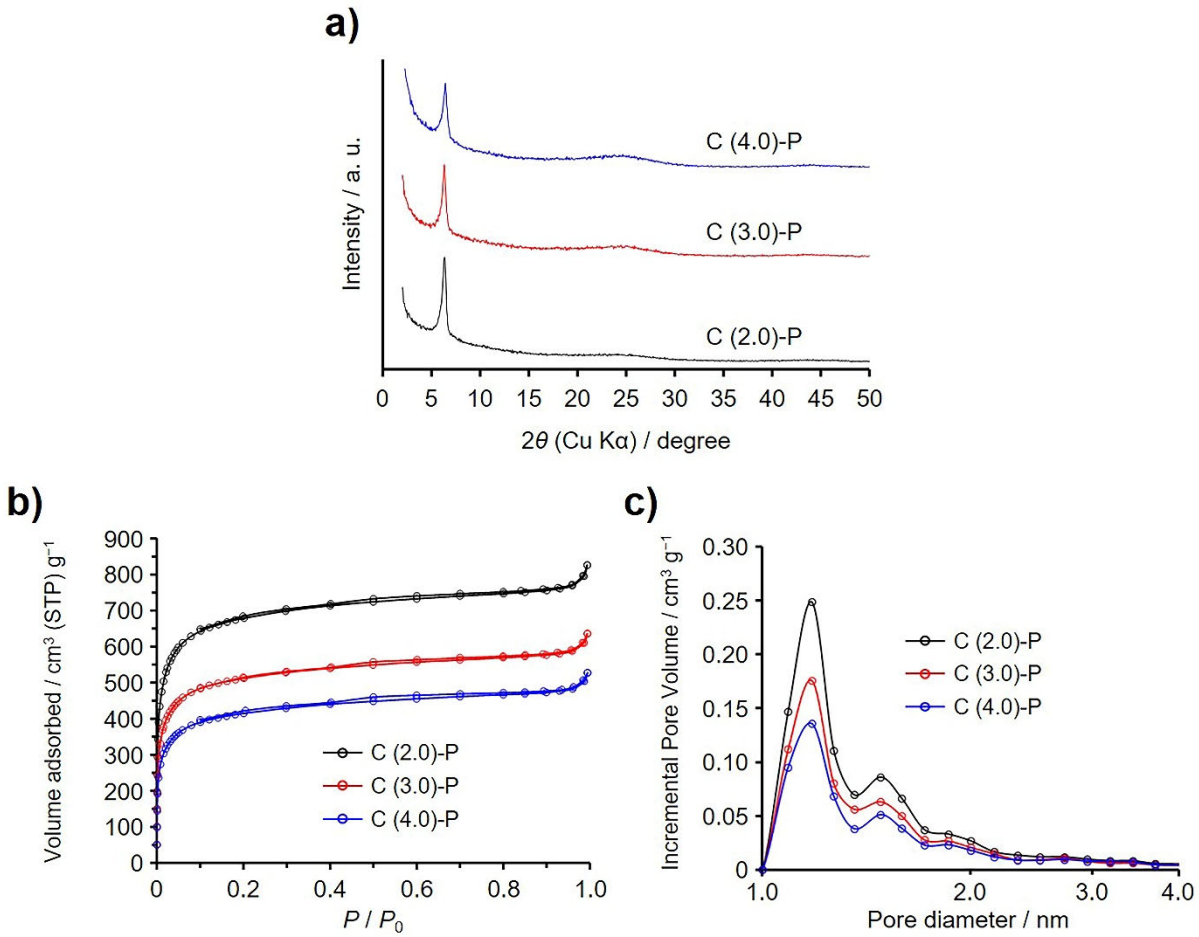

Fig. S6 Results of structural analyses on C (2.0)-P, C (3.0)-P, and C (4.0)-P. (a) XRD patterns. (b) N_2 adsorption/desorption isotherms. (c) Pore size distributions calculated by the DFT method (N_2, −196 °C, carbon slit pore model).

Table S3 BET Specific Surface Areas, Pore Volumes, and Carbon Fractions of ZTCs Prepared Using Propylene and Excess Chitin

Samples	S_{BET} ($m^2\ g^{-1}$)	V_{total} ($cm^3\ g^{-1}$)	V_{micro} ($cm^3\ g^{-1}$)	V_{meso} ($cm^3\ g^{-1}$)	Carbon fraction ($g\ g_{NaY}^{-1}$)
C (2.0)-P	2630	1.19	1.10	0.09	0.424
C (3.0)-P	1980	0.91	0.82	0.09	0.567
C (4.0)-P	1590	0.75	0.66	0.09	0.791

S7. SEM images of chitin and the heated chitins with and without propylene CVD

Fig. S7a shows the SEM image of chitin while Fig. S7b and c present the SEM images of the heated chitins with and without propylene CVD, respectively (for details, see Section S5). No structural change was observed in the SEM image of the heated chitin (Fig. S7b) compared to the unheated chitin (Fig. S7a). Therefore, chitin decomposed without melting, forming micropores and mesopores in the process, as shown in Fig. S5a. The formation of micropores and mesopores mainly proceeds below 500 °C for chitin,[1] while propylene CVD was performed at 700 °C. Therefore, the resulting micropores and mesopores were filled with carbon during propylene CVD for the heated chitin subjected to propylene CVD (Fig. S5a). However, the structural change was not observed between the heated chitins with and without propylene CVD (Fig. S7b and c).

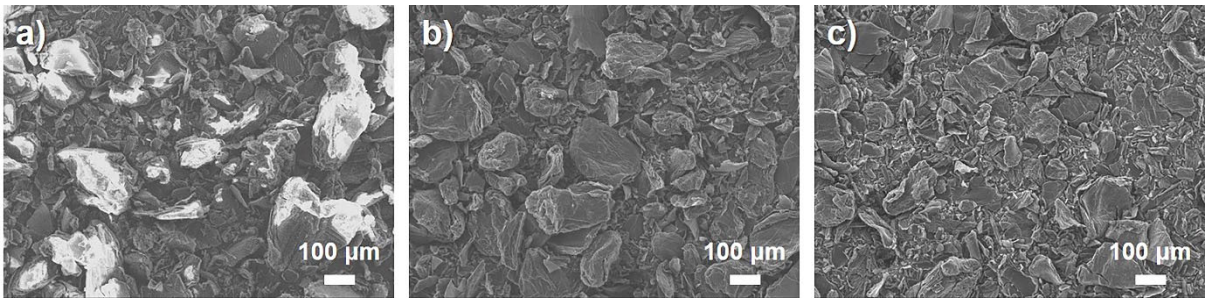

Fig. S7 SEM images of (a) chitin, (b) heated chitin, and (c) chitin subjected to propylene CVD.

S8. Structural characterizations of undoped ZTC

Fig. S8 presents the results of the structural characterizations for the undoped original ZTC. The synthetic method is described in our previous work.[2] The BET specific surface area of the ZTC was 3700 m^2 g^{-1} and the total and micropore volumes were 1.60 and 1.55 cm^3 g^{-1}, respectively.

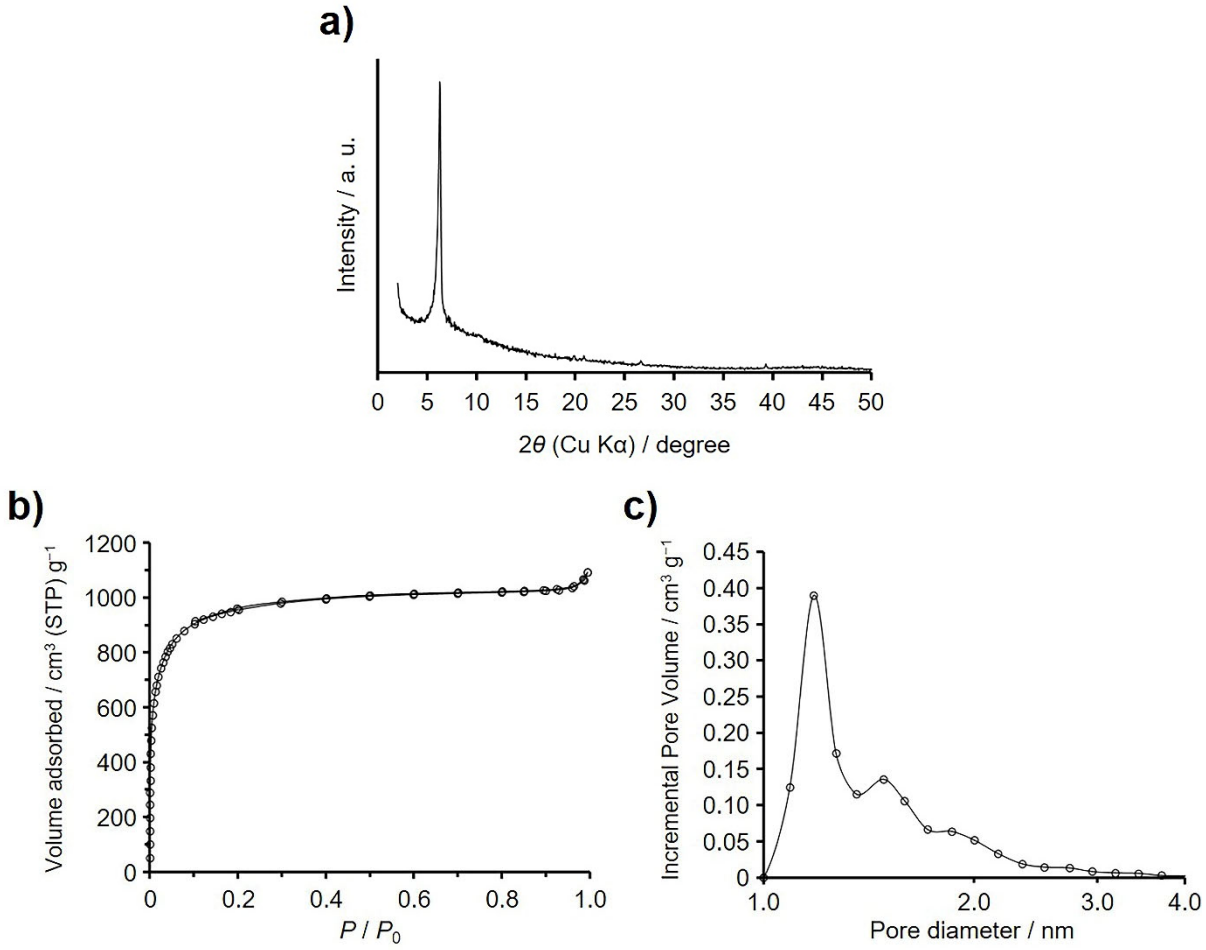

Fig. S8 Results of structural analyses on the undoped original ZTC. (a) XRD patterns. (b) N_2 adsorption/desorption isotherms. (c) Pore size distributions calculated by the DFT method (N_2, −196 °C, carbon slit pore model).

S9. Fitting parameters of Nyquist plots

Fig. S9 shows the fitting results of the Nyquist plots for the ZTCs, using the model depicted in the inset of Fig. 5b. The fitting parameters are summarized in Table S4. As demonstrated in Fig. S9, the fitting results align well with the experimental data.

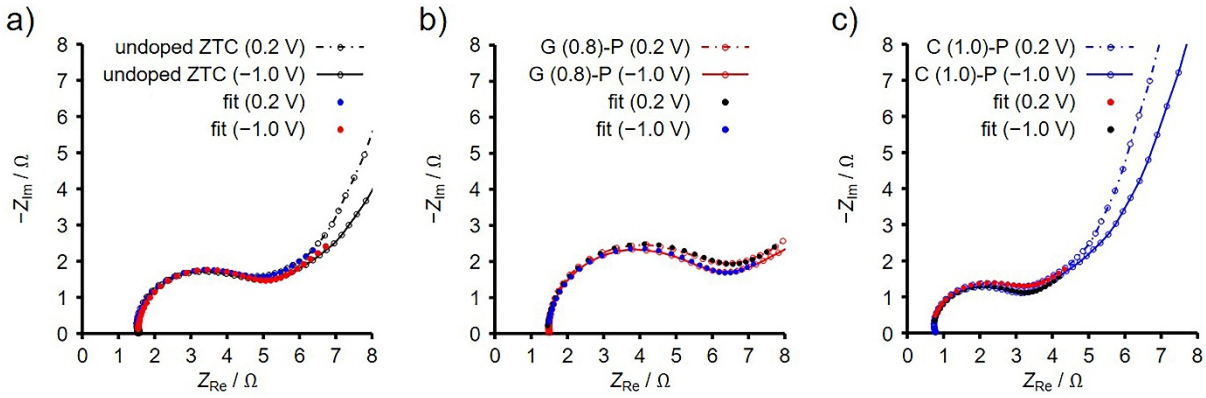

Fig. S9 Fitting results of the Nyquist plots for (a) ZTC, (b) G (0.8)-P, and (c) C (1.0).

Table S4 Fitting Parameters of the ZTCs

Sample	Potential (V)	Fitting parameter			
		R_s (Ω)[a]	R_{ct} (Ω)[b]	C_{dl} (F)[c]	W (Ω $s^{-1/2}$)[d]
undoped ZTC	−1.0	1.5	3.1	2.7×10^{-3}	3.6
	0.2	1.5	3.0	2.7×10^{-3}	4.0
G (0.8)-P	−1.0	1.5	4.3	2.5×10^{-3}	3.4
	0.2	1.4	4.4	2.4×10^{-3}	4.0
C (1.0)-P	−1.0	0.7	2.3	3.4×10^{-3}	2.9
	0.2	0.7	2.3	3.3×10^{-3}	3.7

[a] Series resistance.

[b] Charge transfer resistance.

[c] Double-layer capacitance.

[d] Warburg impedance.

Reference

1. Itoi, H.; Saeki, G.; Usami, T.; Takagi, S.; Suzuki, H.; Ishii, T.; Iwata, H.; Ohzawa, Y., Activation-Free Synthesis of Chitin-Derived Porous Carbon: Application for Electrical Energy Storage. *ACS Sustainable Resour. Manage.* **2024**, 1 (4), 743-756.
2. Itoi, H.; Nishihara, H.; Kogure, T.; Kyotani, T., Three-dimensionally arrayed and mutually connected 1.2-nm nanopores for high-performance electric double layer capacitor. *J. Am. Chem. Soc.* **2011,** *133* (5), 1165-7.